Rotor Position Estimation of PMSM at Low Speed and Standstill Based on the "INFORM" Method

R.G. Segovia, A. Fenollosa and T. Thangamani
Aalborg University, School of Engineering and Science, Pontoppidanstræde 111, DK-9220 Aalborg East, Denmark

***Abstract*— The modern trend of electrical machines is inclined towards permanent magnet synchronous motors (PMSMs). The PMSM has excellent features such as high torque density, high efficiency, high reliability, low maintenance cost, which makes them a dominant player in electric drives. These PMSMs need the rotor position to enable field-oriented control (FOC), which are usually done with mechanical sensors which not only increases costs but also decreases the reliability of the system. Hence the "INFORM" method based rotor position estimation by inductance measurement is analysed as a base to sensor-less control of PMSM. In this method a high frequency voltage injection is used to estimate rotor position and control the machine at low speed.**

I. Introduction

Field Oriental Control (FOC) is commonly used in advanced Permanent Magnet Synchronous Machine (PMSM) drive system with high dynamic performance and efficiency. In order to implement FOC, accurate rotor position is required [1]. During the last few years, sensorless control has become an industry standard as it usually offers more reliable and less expensive solutions in comparison with encoders [2] [3]. An example would be a modern washing machine, where it is quite common to find a Permanent Magnet Synchronous Machine (PMSM) controlled via Field Oriented Control (FOC) with a sensorless control implementation. The system performance without position sensor largely depends on the rotor position estimation, hence the study on different methods of position estimation evolving in various aspects. Consequently, this article discusses one of several methods that exist regarding sensorless control of a PM machine in the low-speed range, which is called the INFORM ("Indirect Flux detection by On-line Reactance Measurement") method.

In the low-speed range the EMF evaluation does not work as this term vanishes. Consequently, this method ensures rotor position detection and thus torque production at standstill. Its principle relies on the magnetic anisotropy of the machine, i.e. magnetic properties that are not independent of the rotor position due to either geometric construction or saturation effects [6]. Thus, the idea is to inject voltages in all three phases (a, b, c) during a very short interval and measure the variation in the current responses. The sum of them results in a complex term, that contains information of the rotor position.

This article analyses the effectiveness of INFORM method in rotor position estimation. Regarding the distribution of the content, it is divided into following parts: Section II, a mathematical explanation and equation used in this method. Section III, the system design and controls are presented. While in Section IV, the implementation of the method in Simulink is shown, where special attention is placed in position estimate analysis of the model. In Section V, the performance of the strategies are evaluated and discussed. While in Section VI, the main conclusions are summarised.

II. Mathematical explanation

The aim of this chapter is to present the mathematical procedure that has been followed to describe the INFORM method. As the real dq-frame is unknown due to the lack of true rotor position, there is only two possible ways to model the machine; work in an estimated $\hat{dq}$-frame or work in the $\alpha\beta$-frame.

However, in order obtain a relationship between these frames and the real dq-frame, the introduction of reference frame transformations is needed. The procedure is as following: The estimated $\hat{dq}$-frame is expressed with respect to the real dq-frame, which is unknown. Once a relationship is established, it is applied as a special case where the estimated $\hat{dq}$-frame corresponds to the $\alpha\beta$-frame, and thus allowing us to obtain a model of the system where the $\alpha\beta$-frame is related with the real dq frame by the real angle (θ_r). This is illustrated and explained into more detail in the next lines.

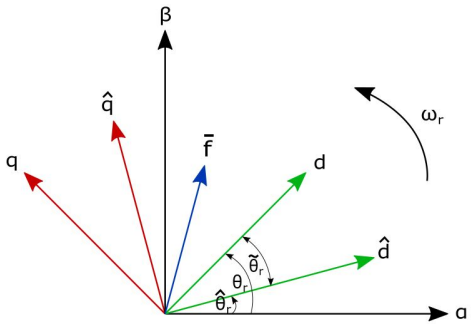

Fig. 1. Graphical relationship between coordinate frames [4].

By using Euler's formulation, and noticing that any vector in the complex plane can be decomposed into its imaginary and real part, i.e. $\bar{f}_{dq} = f_d + jf_q$, then the coordinate frame

expressed in the estimated $\hat{dq}$ axes can be written as:

$$\hat{\bar{f}}_{dq} = \bar{f}_{dq} \cdot e^{j\tilde{\theta}_r} \tag{1}$$

$$\begin{bmatrix} \hat{f}_d \\ \hat{f}_q \end{bmatrix} = \begin{bmatrix} cos(\tilde{\theta}_r) & -sin(\tilde{\theta}_r) \\ sin(\tilde{\theta}_r) & cos(\tilde{\theta}_r) \end{bmatrix} \begin{bmatrix} f_d \\ f_q \end{bmatrix} = K_{er} \begin{bmatrix} f_d \\ f_q \end{bmatrix} \tag{2}$$

Similarly, in the opposite case:

$$\bar{f}_{dq} = \hat{\bar{f}}_{dq} \cdot e^{-j\tilde{\theta}_r} \tag{3}$$

$$\begin{bmatrix} f_d \\ f_q \end{bmatrix} = \begin{bmatrix} cos(\tilde{\theta}_r) & sin(\tilde{\theta}_r) \\ -sin(\tilde{\theta}_r) & cos(\tilde{\theta}_r) \end{bmatrix} \begin{bmatrix} \hat{f}_d \\ \hat{f}_q \end{bmatrix} = K_{re} \begin{bmatrix} \hat{f}_d \\ \hat{f}_q \end{bmatrix} \tag{4}$$

Where the "error" angle ($\tilde{\theta}_r$) is the difference between the real and the estimated angle, as it is displayed in Figure 1. The original voltage Equation expressed in the dq axes is [5]:

$$\bar{v}_{dq} = R\bar{i}_{dq} + \frac{d}{dt}\bar{\lambda}_{dq} + \omega_r \begin{bmatrix} 0 & -1 \\ 1 & 0 \end{bmatrix} \begin{bmatrix} \lambda_d \\ \lambda_q \end{bmatrix} \tag{5}$$

Where:

$$\begin{bmatrix} \lambda_d \\ \lambda_q \end{bmatrix} = \begin{bmatrix} L_d & 0 \\ 0 & L_q \end{bmatrix} \begin{bmatrix} i_d \\ i_q \end{bmatrix} + \begin{bmatrix} \lambda_m \\ 0 \end{bmatrix} \tag{6}$$

Therefore, the estimated $\hat{\bar{\lambda}}_{dq}$ is [5]:

$$\hat{\bar{\lambda}}_{dq} = K_{er}\bar{\lambda}_{dq} = \tag{7}$$

$$\begin{bmatrix} L_1 + L_2 cos(2\tilde{\theta}_r) & L_2 sin(2\tilde{\theta}_r) \\ L_2 sin(2\tilde{\theta}_r) & L_1 - L_2 cos(2\tilde{\theta}_r) \end{bmatrix} \begin{bmatrix} \hat{i}_d \\ \hat{i}_q \end{bmatrix} + \begin{bmatrix} cos(\tilde{\theta}_r)\lambda_m \\ sin(\tilde{\theta}_r)\lambda_m \end{bmatrix} \tag{8}$$

Where:

$$L_1 = \frac{L_d + L_q}{2} \quad , \quad L_2 = \frac{L_d - L_q}{2} \tag{9}$$

Now, if both sides of Equation 5 is multiplied by the transformation matrix K_{er},

$$\hat{\bar{v}}_{dq} = R\hat{\bar{i}}_{dq} + K_{er}\frac{d}{dt}\bar{\lambda}_{dq} + \omega_r \begin{bmatrix} 0 & -1 \\ 1 & 0 \end{bmatrix} \begin{bmatrix} \hat{\lambda}_d \\ \hat{\lambda}_q \end{bmatrix} \tag{10}$$

It is interesting to notice that the second term on the right hand side of Equation 10 can be rewritten as:

$$K_{er}\frac{d}{dt}\bar{\lambda}_{dq} = \frac{d}{dt}\left(K_{er}\bar{\lambda}_{dq}\right) - \frac{d}{dt}(K_{er})K_{re}K_{er}\bar{\lambda}_{dq} \tag{11}$$

$$= \frac{d}{dt}\hat{\bar{\lambda}}_{dq} - \tilde{\omega}_r \begin{bmatrix} 0 & -1 \\ 1 & 0 \end{bmatrix} \hat{\bar{\lambda}}_{dq} \tag{12}$$

Where the introduction of K_{re} and K_{er} in the last part of the previous Equation is valid as its product is unity. This allows Equation 10 to be rewritten as:

$$\hat{\bar{v}}_{dq} = R\hat{\bar{i}}_{dq} + \frac{d}{dt}\hat{\bar{\lambda}}_{dq} + \hat{\omega}_r \begin{bmatrix} 0 & -1 \\ 1 & 0 \end{bmatrix} \begin{bmatrix} \hat{\lambda}_d \\ \hat{\lambda}_q \end{bmatrix} \tag{13}$$

By comparing Equations 5 and 13, one can notice that the estimated voltage Equation and the original voltage Equation look similar. However, in the actual one, the flux linkage Equations in the d and q axes are decoupled, whereas in the estimated one they are coupled, unless $\tilde{\theta}_r = 0$.This is interesting, as it could be used as an estimator for the position error, although it is not further discussed here.

Anyway, Equations 7 and 13 can be further expanded. Starting with Equation 13:

$$\hat{\bar{v}}_{dq} = R\hat{\bar{i}}_{dq} + \frac{d}{dt}\hat{\bar{\lambda}}_{dq} + \hat{\omega}_r \begin{bmatrix} 0 & -1 \\ 1 & 0 \end{bmatrix} \begin{bmatrix} \hat{\lambda}_d \\ \hat{\lambda}_q \end{bmatrix} \tag{14}$$

$$= R\hat{\bar{i}}_{dq} + \frac{d}{dt}\hat{\bar{\lambda}}_{dq} + \hat{\omega}_r(-\hat{\lambda}_q + j\hat{\lambda}_d) \tag{15}$$

$$= R\hat{\bar{i}}_{dq} + \frac{d}{dt}\hat{\bar{\lambda}}_{dq} + j\hat{\omega}_r(\hat{\lambda}_d + j\hat{\lambda}_q) \tag{16}$$

$$= R\hat{\bar{i}}_{dq} + \frac{d}{dt}\hat{\bar{\lambda}}_{dq} + j\hat{\omega}_r\hat{\lambda}_{dq} \tag{17}$$

And for Equation 7:

$$\hat{\bar{\lambda}}_{dq} = \begin{bmatrix} L_1 + L_2 cos(2\tilde{\theta}_r) & L_2 sin(2\tilde{\theta}_r) \\ L_2 sin(2\tilde{\theta}_r) & L_1 - L_2 cos(2\tilde{\theta}_r) \end{bmatrix} \begin{bmatrix} \hat{i}_d \\ \hat{i}_q \end{bmatrix} \tag{18}$$

$$+ \begin{bmatrix} cos(\tilde{\theta}_r)\lambda_m \\ sin(\tilde{\theta}_r)\lambda_m \end{bmatrix} \tag{19}$$

$$= L_1(\hat{i}_d + j\hat{i}_q) + L_2(\hat{i}_d \cos 2\tilde{\theta}_r + \hat{i}_q \sin 2\tilde{\theta}_r \tag{20}$$

$$+ j\hat{i}_d \sin 2\tilde{\theta}_r - j\hat{i}_q \cos 2\tilde{\theta}_r) + \lambda_m e^{j\tilde{\theta}_r} \tag{21}$$

$$= L_1\hat{\bar{i}}_{dq} + L_2(\hat{i}_d - j\hat{i}_q)(\cos 2\tilde{\theta}_r + j \sin 2\tilde{\theta}_r) \tag{22}$$

$$+ \lambda_m e^{j\tilde{\theta}_r} \tag{23}$$

$$= L_1\hat{\bar{i}}_{dq} + L_2\hat{\bar{i}}^*_{dq}e^{j2\tilde{\theta}_r} + \lambda_m e^{j\tilde{\theta}_r} \tag{24}$$

This Equation is differentiated, as a requirement for Equation 14.

$$\frac{d\hat{\bar{\lambda}}_{dq}}{dt} = L_1\frac{\hat{\bar{i}}_{dq}}{dt} + L_2\frac{\hat{\bar{i}}^*_{dq}}{dt}e^{j2\tilde{\theta}_r} + j2\tilde{\omega}_r L_2\hat{\bar{i}}^*_{dq}e^{j2\tilde{\theta}_r} \tag{25}$$

$$+ j\tilde{\omega}_r\lambda_m e^{j2\tilde{\theta}_r} \tag{26}$$

Therefore, Equation 14 can be rewritten as:

$$\hat{\bar{v}}_{dq} = R\hat{\bar{i}}_{dq} + L_1\frac{\hat{\bar{i}}_{dq}}{dt} + L_2\frac{\hat{\bar{i}}^*_{dq}}{dt}e^{j2\tilde{\theta}_r} \tag{27}$$

$$+ j2\tilde{\omega}_r L_2\hat{\bar{i}}^*_{dq}e^{j2\tilde{\theta}} + j\tilde{\omega}_r\lambda_m e^{j2\tilde{\theta}} + j\hat{\omega}_r\hat{\lambda}_{dq} \tag{28}$$

For the special case when $\hat{\theta}_r$ and $\hat{\omega}_r$ are zero, that is, when it represents the $\alpha\beta$ reference frame, the voltage Equation becomes:

$$\bar{v}_{\alpha\beta} = R\bar{i}_{\alpha\beta} + L_1\frac{\bar{i}_{\alpha\beta}}{dt} + L_2\frac{\bar{i}^*_{\alpha\beta}}{dt}e^{j2\theta_r} \tag{29}$$

$$+ j2\tilde{\omega}_r L_2\bar{i}^*_{\alpha\beta}e^{j2\theta_r} + j\tilde{\omega}_r\lambda_m e^{j2\theta_r} \tag{30}$$

As $\hat{\theta}_r$ is equal to zero, $\tilde{\theta}_r = \theta_r - \hat{\theta}_r = \theta_r$. This represents the voltage Equation in the $\alpha\beta$ axes, which contains position information of the real dq axis, by the angle θ_r. This information appears in the back-EMF term and it is also linked with the inductances L_d and L_q, from L_2.
However, in the low-speed range, when w_r is close to zero, the term containing the back-EMF approaches to zero. This means the position information is only related to the

inductances. The resulting voltage Equation in the low-speed range is approximated by:

$$\bar{v}_{\alpha\beta} = L_1 \frac{d\bar{i}_{\alpha\beta}}{dt} + L_2 \frac{d\bar{i}^*_{\alpha\beta}}{dt} e^{j2\theta_r} \tag{31}$$

As the supplied voltage can be controlled, the previous Equation is isolated for the current $\bar{i}_{\alpha\beta}$, leading to:

$$\triangle\bar{i}_{\alpha\beta} = \left(\frac{L_1}{L_1^2 - L_2^2} + \frac{-L_2}{L_1^2 - L_2^2} e^{j2(\theta_r - \theta_v)} \right) \triangle t \cdot \bar{v}_{\alpha\beta} \tag{32}$$

$$= \left(y + \triangle y e^{j2(\theta_r - \theta_v)} \right) \triangle t \cdot V_m e^{j\theta_v} \tag{33}$$

$$= y\triangle t V_m e^{j\theta_v} + \triangle y \triangle t V_m e^{j(2\theta_r - \theta_v)} \tag{34}$$

Where:

$$\frac{d\bar{i}_{\alpha\beta}}{dt} \approx \frac{\triangle\bar{i}_{\alpha\beta}}{\triangle t} \quad , \quad \bar{v}_{\alpha\beta} = V_m e^{j\theta_v} \tag{35}$$

It is in this point where, in order to obtain the position information, the INFORM method is introduced. By looking at Equation 32, it is clear that somehow the first term (the ones that contains the component y) should be removed. The procedure for this method is to inject three voltage vectors aligned with phases a, b and c, which are separated by 120^o electrical. This is seen below:

$$\triangle\bar{i}_{\alpha\beta 1} = y\triangle t V_m e^{j0^o} + \triangle y \triangle t V_m e^{j(2\theta_r)} \tag{36}$$

$$\triangle\bar{i}_{\alpha\beta 2} = y\triangle t V_m e^{j120^o} + \triangle y \triangle t V_m e^{j(2\theta_r - 120^o)} \tag{37}$$

$$\triangle\bar{i}_{\alpha\beta 3} = y\triangle t V_m e^{j240^o} + \triangle y \triangle t V_m e^{j(2\theta_r - 240^o)} \tag{38}$$

These Equations are multiplied by its corresponding the exponential of the angle of its phase:

$$\triangle\bar{i}_{\alpha\beta 1} e^{j0^o} = y\triangle t V_m e^{j0^o} e^{j0^o} + \triangle y \triangle t V_m e^{j(2\theta_r)} \tag{39}$$

$$\triangle\bar{i}_{\alpha\beta 2} e^{j120^o} = y\triangle t V_m e^{j120^o} e^{j120^o} + \triangle y \triangle t V_m e^{j(2\theta_r)} \tag{40}$$

$$\triangle\bar{i}_{\alpha\beta 3} e^{j240^o} = y\triangle t V_m e^{j240^o} e^{j240^o} + \triangle y \triangle t V_m e^{j(2\theta_r)} \tag{41}$$

Summing all these together:

$$\bar{A} = \triangle\bar{i}_{\alpha\beta 1} + \triangle\bar{i}_{\alpha\beta 2} + \triangle\bar{i}_{\alpha\beta 3} \tag{42}$$

$$= 3\triangle y \triangle t V_m e^{j(2\theta_r)} \tag{43}$$

The first term on each Equation disappears when summed, as the sum of $e^{j0^o} + e^{j120^o} + e^{j240^o}$ is zero. Therefore, the component y is no longer present in the Equation. Now, the position information can be easily found:

$$\frac{Im(\bar{A})}{Re(\bar{A})} = \tan(2\theta_r) \tag{44}$$

Therefore, the angle θ_r is:

$$\theta_r = \frac{atan2(\frac{Im(\bar{A})}{Re(\bar{A})})}{2} \tag{45}$$

When dividing the angle by two, the range becomes from [-90, 90], instead of from [-180, 180], but this is something unavoidable when performing this method [6].

III. Control Scheme

The project estimates the rotor angle of the PMSM using the angle calculation, as stated already only double the desired angle can be obtained from the described procedure. Hence, to recover the entire angle spectrum a a simple control scheme is implemented where the system holds the previous value of angle and compares it with the current estimate and outputs an angle which resonates the actual rotor angle of the machine. A flowchart of the operation is displayed in Figure 2.

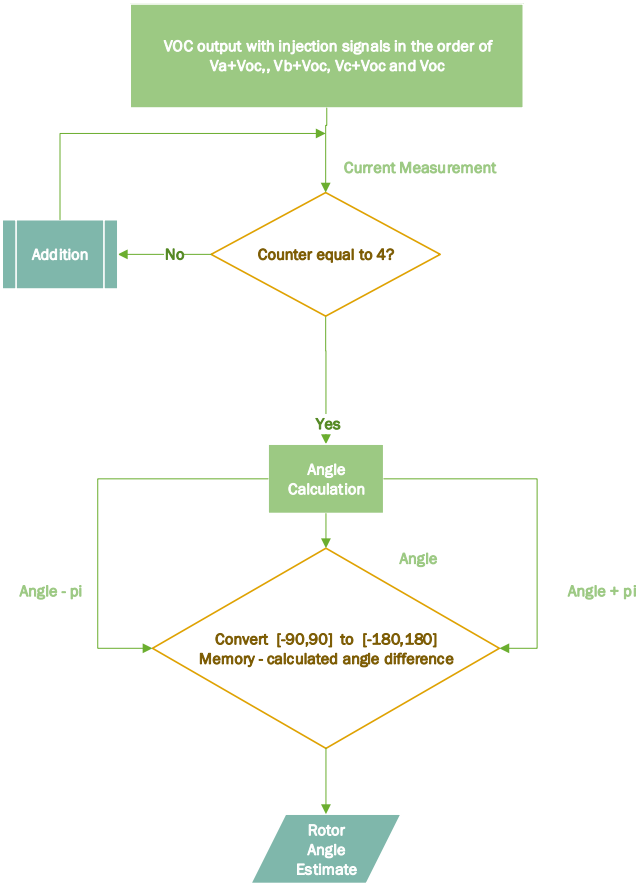

Fig. 2. Rotor position estimate calculation.

The input signals combined with the FOC are injected into the system using a multiport switch, with its switching sequence synchournised with the sampling frequency of the system, controlled by a free running counter. This counter also acts as a pointer for the sequence of injection to calculate the measured current as a vector and perform the required calculation. As displayed in the flow chart the strategy to obtain a estimate rotor position similar to the actual one, three difference signal are generated based on the estimated angle, angle plus π and angle minus π in correspondence to the previous sampling time rotor estimate. A set of conditional statements are run, based on the objective of

providing a robust rotor angle position. If difference output satisfies the condition of staying within the range of 1 and -1 its corresponding output is the estimated rotor angle.

IV. Simulation

An overview of system configuration implemented to estimate and verify sensorless control using INFORM method is based on Figure 3.

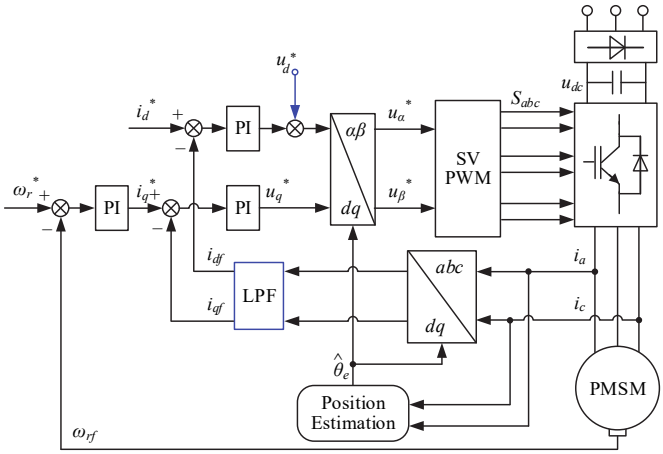

Fig. 3. System configuration for implementation of INFORM [7].

The study of rotor position estimation is done with a mathematical model of a 7 kW PMSM with FOC implemented within the system. The parameters of the motors are displayed in the Table I.

TABLE I
Machine Parameters

Parameter	Discription	Value
Vs	Max. RMS phase voltage	360 [V]
nrat	Rate speed	1750 [rpm]
Npp	Number of pole pairs	4
Lndmpm	Rotor peak PM flux linkage	0.412 [web.turns]
J	Motor inertia	1e-3 [J.m^2]
Trat	Rated torque	38 [Nm]
fs	Switching frequency	10e3 [Hz]
Rs	Motor resistance	0.78 [ohm]
Lls	Leakage inductance	2e-3 [H]
Ld	d - axis inductance	10e-3 [H]
Lq	q - axis inductance	12.8e-3 [H]

Different simulations are carried out in Simulink, to access the feasibility of this method. The simulations can be classified into two different parts:

- A simulation with the real angle provided by the motor model.
- A simulation with the estimated angle provided by the INFORM method.

In the first part, a comparison between the real angle and the estimated angle is done at various speed of 10, 100, 500 and 1000 [rpm]. In the second part, the viability of this method to control the motor is checked for speeds of 100 and 500 [rpm].

In order to compare the results between the different simulations, the load torque is kept constant in all studies as displayed in Figure 4; the torque load is zero during the first two seconds, then the rated torque is applied and, finally, after four seconds, the load returns to zero.

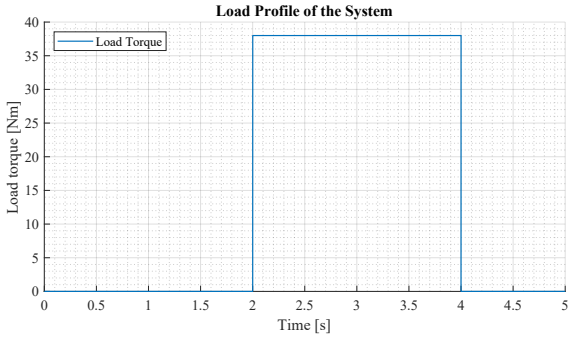

Fig. 4. Load torque applied to the motor.

V. Results and Discussion

During the study case analysis of angle estimation the motor is analysed with a speed variation of 10, 100, 500 and 1000 individually.

A. Real angle as input

1) ***10 rpm****:* As it has been explained in this paper, the INFORM method provides a good estimation of the angle at standstill operation of the machine. For this reason, accuracy in the estimated angle is expected. The results is displayed in Figure 5.

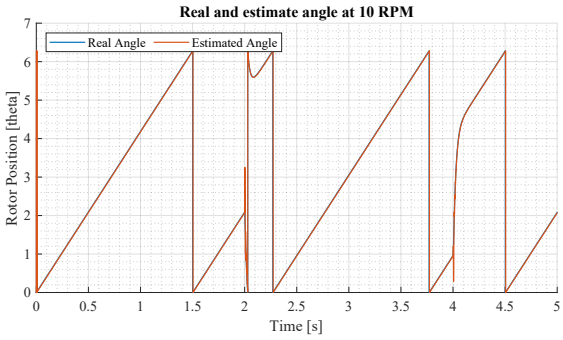

Fig. 5. Angle Comparison at 10 RPM.

The speed of the machine is displayed in Figure 6. Some irregularities can be seen when the torque is applied, which is something expected. Furthermore, as the estimated angle is not used in this first part of the experimentation, the speed plots is not provided for the upcoming speeds rates, as no changes are expected on the graph.

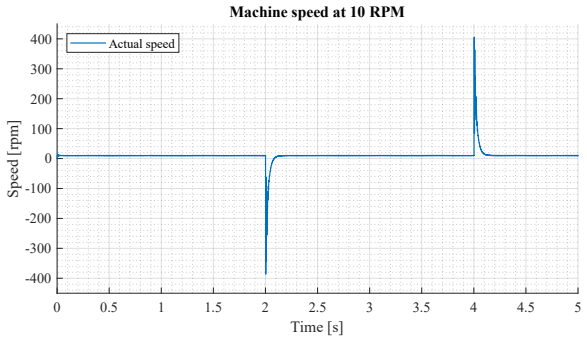

Fig. 6. speed at 10 RPM.

*2) **100 rpm**:* With the increase in speed, small errors and variations in the angle is expected, as it can be seen in the results for simulation in the Figure 7. Nevertheless, the trajectory of the real angle is followed by the estimated angle, even when the rated load is applied.

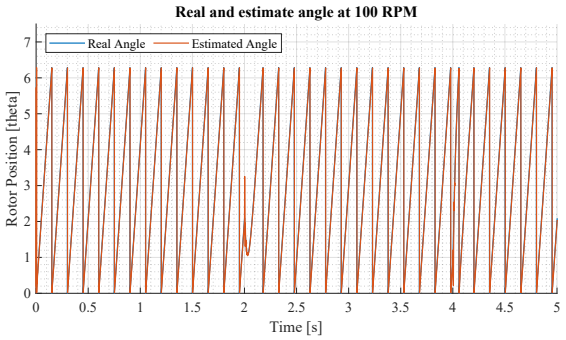

Fig. 7. Angle difference at 100 RPM.

A closer look at the results displays a small error in the angle is found in Figure 8.

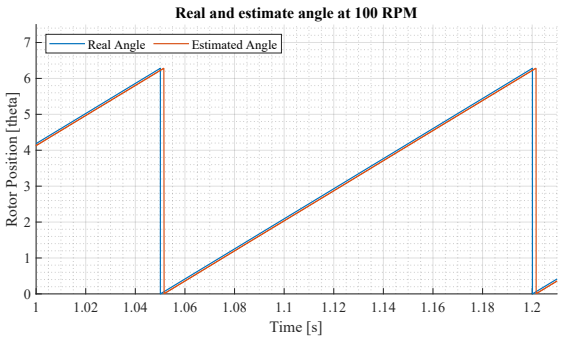

Fig. 8. Angle difference at 100 RPM.

*3) **500 rpm**:* At 500 [rpm] speed, the accuracy of the estimate in the system is no longer providing a good solution to the FOC. This delay between the real angle and the estimated angle is displayed in Figure 9.

At this point, the viability of this method will depend on the application.

*4) **1000 rpm**:* As expected, a totally erratic angle is given at this speed. This is displayed in Figure 10.

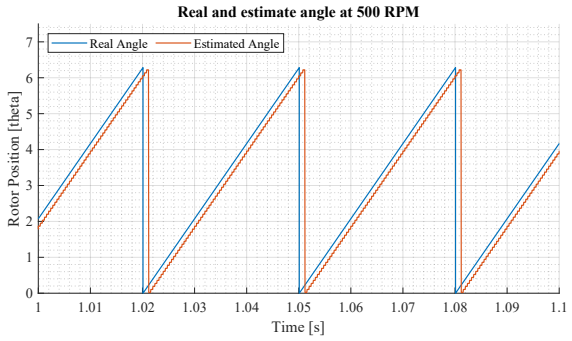

Fig. 9. Angle difference at 500 RPM.

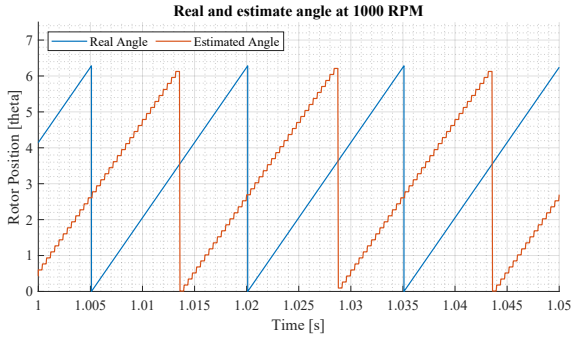

Fig. 10. Angle difference at 1000 RPM.

B. Estimated angle as input

Once the estimation accuracy of the angle was found in the previous part, the estimated angle is now used as an input for the FOC control loop to finally check the viability of this method. In Figure 11 the speed of the machine at 100 [rpm] is simulated. As displayed, the speed is kept constant within the range of 100 rpm as desired. Small disturbances are discovered at T = 2 [s] and T = 4 [s] as the torque load change at these two moments.

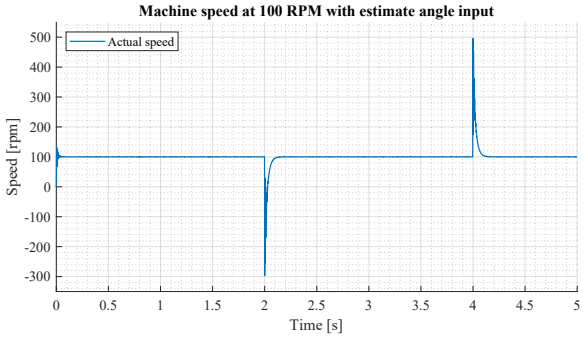

Fig. 11. Speed at 100 RPM with estimated angle as input.

In order to analyze the performance of the angle inputted to the FOC, the angle graph is displayed in Figure 12. Furthermore, the estimated angle follows the real one as it is forced to do it by using the estimated angle as an input for this loop.

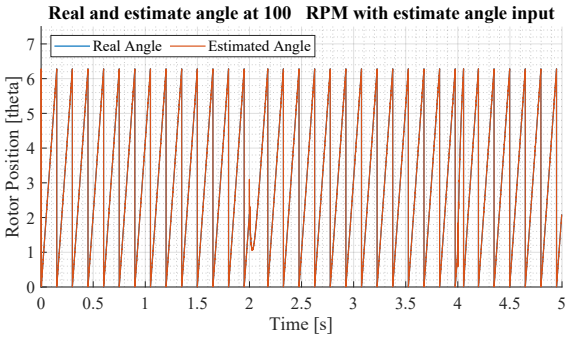

Fig. 12. Angle difference at 100 RPM with estimated angle as input.

If the speed of the machine is increased to 500 [rpm], the FOC is not able to keep a constant speed at this reference value. Once a torque load is applied to the motor, the system becomes unstable.

VI. Conclusion

Throughout this article, the concepts and viability of the INFORM method is presented. The mathematical part showed the formulation and the idea behind this method. A mathematical based machine was developed and used to implement the required injection strategy to verify the feasibility of INFORM method. The INFORM Method had a better performance at lower speeds, being ideal for standstill application. This statement was verified using simulation techniques in the Simulink software solution IV.

Furthermore, as displayed in chapter V, as the speed increases, a delay between the estimated angle and the real angle is found. This delay produces the inability to apply this method to control the motor at high speeds. In position-controlled mode, the limits of the INFORM method concerning angular accuracy are analysed and the sensorless estimation of the angle effectively tracks the real angle of the rotor for various low-speed cases. Furthermore, when using the estimated angle as input to the FOC, the control system provides a satisfactory results when the reference speed is low.

VII. License

References

[1] R. Ni, D. Xu, G. Wang, L. Ding, G. Zhang, and L. Qu, “Maximum Efficiency Per Ampere Control of Permanent-Magnet Synchronous Machines,” IEEE Trans. Ind. Electron., vol. 62, no. 4, pp. 2135-2143, 2015.

[2] Rajashekara, K., Kawamura, A., Matsuse, K., "Sensorless control of AC motor dnves", IEEE Press, 1996

[3] Sepe, R.B., Lang, J.H., "Real-time observer-based (adaptive) control of a permanent-magnet synchronous motor without mechanical sensor", IEEE Trans. Ind. Appl., Vol. 28, No. 6, pp. 1345-1352, 1992.

[4] P. L. Chapman and S. D. Sudhoff, A multiple reference frame synchronous estimator/regulator, IEEE Trans. Energy Conversion, 15(2), 197–202, 2000.

[5] W. Leohnard, Control of Electric Drives, 2nd ed., Springer-Verlag, New York, 1997.

[6] M. Schroedl, "Sensorless control of AC machines at low speed and standstill based on the “INFORM” method", Conference Record of the 1996 IEEE Industry Applications Conference 1996.

[7] N. Ronggang, L. Kaiyuan, F. Blaabjerg, D. Xu, "A comparative study on pulse sinusoidal high frequency voltage injection and INFORM methods for PMSM position sensorless control", IECON 2016–42nd Annu. Conf. IEEE Ind. Electron. Soc., pp. 2600-2605, 2016.